Methamphetamine modulates the production of interleukin-6 and tumor necrosis factor-alpha *via* the cAMP/PKA/CREB signaling pathway in lipopolysaccharide-activated microglia

Biao Wang[a], Teng Chen[b], Jing Wang[a], Yuwei Jia[a], Huixun Ren[a], Feng Wu[c], Mei Hu[d], Yanjiong Chen[a,*]

[a] Department of Immunology and Pathogenic Biology, College of Basic Medicine, Xi'an Jiaotong University Health Science Center, Xi'an 710061, China
[b] Forensic Medicine College of Xi'an Jiaotong University, Key Laboratory of the Health Ministry for Forensic Medicine, Xi'an 710061, China
[c] Graduate Teaching and Experiment Centre, Xi'an Jiaotong University Health Science Center, Xi'an 710061, China
[d] Editorial Department of Infectious Disease Information, 302 Hospital of PLA, Beijing 100039, China

ARTICLE INFO

ABSTRACT

Methamphetamine (METH) elicits neuroinflammatory effects that may implicate its regulatory role on the microglial immune response. However, the mechanism underlying this remains unclear. In the present study, the effects of METH on lipopolysaccharide (LPS)-induced interleukin-6 (IL-6) and tumor necrosis factor-alpha (TNF-α) productions were tested in BV-2 cells and primary microglial cells. Additionally, western blot analysis was used to examine the phosphorylation of mitogenactivated protein kinases (MAPKs). Next, we detected the alterations in cAMP content and the phosphorylation levels of CREB in microglial cells to determine the involvement of the cAMP/CREB signaling pathway. We also used an adenylyl cyclase (AC) agonist (forskolin) and antagonist (MDL-12330A) and a PKA antagonist (H89) to confirm their participation. We observed that METH alone did not affect the production of IL-6 or TNF-α. In contrast, METH augmented the IL-6 production and inhibited the TNF-α production induced by LPS. A similar effect of forskolin was also observed in BV-2 cells. While MAPK activation was not influenced by METH alone, the LPS-induced phosphorylation p38, JNK and ERK1/2 were all reduced by METH. Both the concentration of cAMP and the phosphorylation of CREB were increased by METH in LPS-activated microglial cells. The effects of METH were altered by MDL-12330A and H89. Moreover, the inhibition of the phosphorylation of ERK1/2 by METH was also reversed. These results suggest that the differential regulation of IL-6 and TNF-α by METH in LPS-activated microglial cells may be attributable to the cAMP/PKA/CREB signaling pathway.

1. Introduction

Methamphetamine (METH) is a popular and highly addictive drug. The abuse of METH causes neurotoxic effects that have resulted in a serious global health problem that accompanied with neuropsychiatric and neuropathological complications [1,2]. METH abuse could change the levels of inflammation in the mouse brain [3,4]. Sustained inflammation further promotes the generation and accumulation of neurotoxic inflammatory mediators that contribute to neural damage in neurodegenerative diseases and psychostimulant drug abuse [5–7]. Microglial cells, which constitute 5–15% of all brain cells, are the resident immune cells in the brain. Microglial cells are involved in immune surveillance in the intact brain and become activated during the course of neurodegeneration [8]. Immune dysfunction in the brain,

primarily caused by sustained activation of microglial cells, plays a significant role in the progression of neurodegeneration diseases, such as Parkinson's disease [9,10]. It is widely known that microglial participation is involved in the cytotoxicity of substances such as METH [11,12]. METH abusers exhibit marked microglial activation in some brain regions, even after two years of abstinence from drug use [13]. Increasing evidences indicate that the neuroinflammation exemplified by microglial activation or changed response intensity plays an important role in METH relevant neurotoxicity [14]. Thus, the study of the regulation on microglial immune response by METH will help us to understand the actual mechanisms underlying its impacts.

To observe the effects of METH on microglia, immortalized murine BV-2 cells, which exhibit both the phenotypic and functional properties of reactive microglial cells, and primary microglia cells were used in

---

present study [15]. Many stimulators, such as interferon-γ (IFN-γ), amyloids and lipopolysaccharide (LPS), can activate microglial cells [5,16,17]. LPS, a component of the outer membrane of gram-negative bacteria, is widely used as an efficient immune stimulus both *in vivo* and *in vitro* [18–22]. When incubated with LPS, both BV-2 cells and primary microglia secrete a series of inflammatory cytokines that include tumor necrosis factor-alpha (TNF-α) and interleukin-6 (IL-6) [23,24]. Both of them are multifunctional cytokines that have a pro-inflammatory role and participate in the promotion and progression of neurological diseases, such as schizophrenia and hepatic encephalopathy [25–28]. The mitogen-activated protein kinases (MAPKs) are a family of signal transduction proteins that include the extracellular signal regulated kinase (ERK1/2), the c-Jun NH2-terminal kinases (JNK), and the p38 isoform (p38) [19,20,29]. The actions of LPS include promoting the phosphorylation of p38, JNK and ERK1/2, which directly result in the generation and secretion of proinflammatory cytokines [19,30]. Hence, it is helpful to examine MAPKs to elucidate the mechanism by which METH regulates inflammatory cytokines. Cyclic adenosine monophosphate (cAMP) is an important second messenger that can be regulated by METH [31,32]. Furthermore, cAMP is also involved in the secretion of inflammatory cytokines [33,34], and its downstream components, protein kinase A (PKA) and cAMP response element binding protein (CREB), have been found to be involved in the modulation of immune function [35]. The role of cAMP signaling in the context of METH-altered neuroinflammation is still not elucidated.

In the current study, we measured the effects of METH on LPS-induced IL-6 and TNF-α production in BV-2 cells and primary microglial cells. In order to address the underlying mechanism, we next examined the activation of MAPKs (p38, JNK and ERK1/2) and the cAMP/CREB signaling pathway during that process. We further used an adenylyl cyclase (AC) agonist (forskolin) and antagonist (MDL-12330A) and a PKA antagonist (H89) to address how this signaling pathway was involved. Our results suggested a contribution of cAMP/PKA/CREB signaling pathway in METH modulated production of cytokines in LPS-activated microglial cells.

2. Materials and methods

2.1. Cells and drugs

BV-2 cells were acquired from Kunming Institute of Zoology in Chinese Academy of Sciences (Kunming, Yunnan, China). RPMI1640 and DMEM/F12 were bought from HyClone (Logan, Utah, USA). Fetal bovine serum was obtained from SiJiQing (Hangzhou, Zhejiang, China). METH (methamphetamine hydrochloride) was purchased from the National Institute for the Control of Pharmaceutical and Biological Products (Beijing, China). LPS (*Escherichia coli*, serotype O55:B5), and MDL-12330A hydrochloride hydrate was purchased from Sigma Aldrich (St. Louis, Missouri, USA). H89 dihydrochloride was bought from Selleck Chemicals (Houston, Texas, USA). Forskolin was purchased from Beyotime Biotechnology (Wuhan, Hubei, China). The enzyme-linked immunosorbent assay kits for the quantitative detection of mouse TNF-α and IL-6 were obtained from eBioscience (San Diego, California, USA). The cyclic AMP ELISA kit was bought from Cayman Chemical (Ann Arbor, Michigan, USA). All of the primary antibodies for p-p38, p38, p-JNK, JNK, p-ERK1/2, ERK1/2, p-CREB, and CREB were purchased from Cell Signaling Technology (Boston, Massachusetts USA). Secondary goat anti-rabbit antibody conjugated with HRP was bought from Abgent (San Diego, USA). The Pierce™ ECL Plus Western Blotting Substrate detection kit was from Thermo Fisher Scientific (Rockford, USA).

The primary microglial cells were derived from the brains of postnatal C57BL/6 J mice as described previously [36]. Briefly, newborn C57BL/6 J mice were chosen for the isolation of brain tissues. The meninges were carefully removed using a dissecting microscope. The tissues were cut into small pieces and then trypsinized for at least

15 min. Dulbecco's modified Eagle's medium (DMEM)/F12 media containing 10% FBS was added to terminate the digestion. The cells were collected by centrifugation at 800 rpm/min for 5 min and then plated into 25 cm² flasks. The medium was replaced every 3 days until 10–15 days to acquire the primary mixed glial cells. The primary microglial cells were harvested by rapid shaking for 1 h in a reciprocal shaker. The purity of microglial cells was detected by CD11b staining with flow cytometry, and 98% pure was considered acceptable for the following experiments. All experiments were performed in accordance with the guidelines of the animal ethics committee of Xi'an Jiaotong University.

2.2. Cell treatments

BV-2 and primary microglial cells were cultured in complete media (RPMI1640 or DMEM/F12 with 10% fetal bovine serum and 1% penicillin–streptomycin). A total of 1.5×10^5 cells per well were plated in 24-well microtiter plates. The cells were treated after 2 h of incubation. METH was diluted in complete media to concentrations of 0, 20, 100, and 200 μM to test the effects of METH alone on the microglial cells. To examine the effects of LPS alone, the LPS it was diluted in complete media to the following concentrations: 10, 100, 500, 1000, and 2000 ng/ml. Subsequently, all LPS concentrations used in this paper were 1000 ng/ml. In the assay that combined METH and LPS, METH was added to the well 10 min prior to LPS. When used, H89 (30 μM), forskolin (10 μM) and MDL-12330A (10 μM) were added 15–30 min before the METH.

2.3. MTT assay

The standard 3-(4, 5-dimethylthiazol-2-yl)-2, 5-diphenyltetra-zolium bromide (MTT) assay was used to assess cell viability. Microglial cells were seeded in 96-well microtiter plates (6×10^4 cells/well) for 2 h and then exposed to the various treatments for 24 h. Next, 20 μl MTT solution (5 mg/ml in phosphate-buffered saline) was added to each well, and the wells were incubated for 4 h at 37 °C. The metabolized MTT product was dissolved in DMSO and quantified by measuring the optical density at 570 nm with reference wavelength at 630 nm. in a microplate reader (Thermo Fisher Scientific, USA).

2.4. Quantitative real-time PCR

Total RNA was extracted and purified from the cells using a TRIzol kit (Invitrogen, Carlsbad, CA, USA). A260/A280 was used to detect the concentration and purity of the RNA in a microplate reader (Thermo Fisher Scientific, USA). Reverse transcription was performed to yield cDNA using a Prime Script TMRT reagent kit (Takara Bio Inc., Shiga, Japan). We chose SYBR Green II as the double-strand DNA-specific binding dye to complete the real-time PCR on a Stratagene Mx 3005p Real-Time PCR Detection System (Agilent Technologies, Santa Clara, CA, USA). The GAPDH gene was used as the loading control gene. All primers were synthesized by Haining Biotech (Xi'an, China). The forward and reverse primers used in the PCR reactions were as follows (all presented as 5′-3′): IL-6, CTGCAAGAGACTTCCATCCAGTT and AGGGAAGGCCGTGGTTGT; TNF-α, GGCTGCCCCGACTACGT and ACTTTCTCCTGGTATGAGATAGCAAAT; GAPDH, TGTGTCCGTCGTGG ATCTGA and TTGCTGTTGAAGTCGCAGGAG. The PCR cycle was as follows: initial step at 95 °C for 30 s, 40 cycles at 95 °C for 5 s and 60 °C for 30 s, 1 cycle at 95 °C for 1 min, 55 °C for 30 s, and 95 °C for 30 s. The specificity of the reaction was verified by melting curve analysis.

2.5. Measurement of cytokines and cAMP

Following an incubation period of 24 h after the addition of METH, the cell supernatants were carefully collected from the 24-well microtiter plates and centrifuged at 3000 rpm/min for 10 min at 4 °C in a
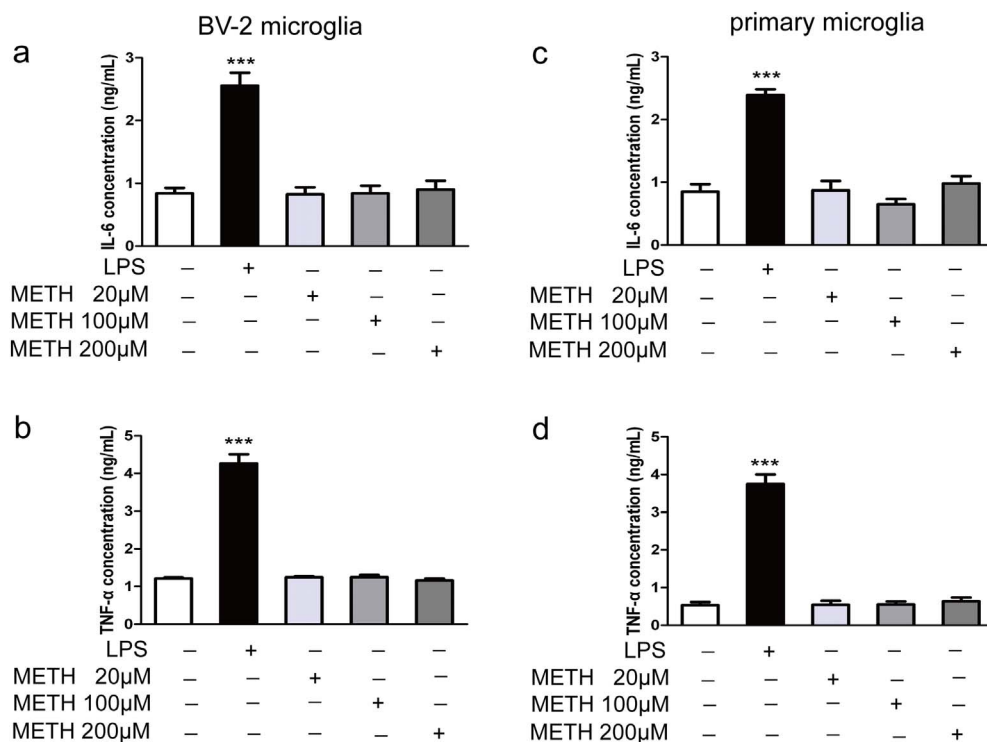
BV-2 microglia

primary microglia

centrifugal machine. The measurements of the concentrations of IL-6 and TNF-α were completed according to the manufacturer's recommendations. The detection limits for IL-6 and TNF-α were 6.5 pg/ml and 3.7 pg/ml, respectively.

After a 15-min incubation with METH, the supernatants were discarded, at which time 1 ml of 0.1 M HCL was added for every 35 cm^2 of surface area for 20 min at room temperature. The cells were collected with cell scrapers and centrifuged at 1000 rpm/min for 10 min to obtain the supernatant. The cAMP content was measured according to the manufacturer's recommendations. The detection limit for cAMP was 0.3 pmol/ml.

2.6. Western blotting

To measure the MAPK phosphorylation levels, single-cell suspensions were plated in 6-well microtiter plates (1×10^6 cells/well). After a 30-min incubation with METH and LPS, the cells were washed three times with pre-cooled phosphate-buffered saline, and the cell extracts were prepared using ice-cold RIPA lysis buffer (Solarbio, China) with 1% protease inhibitor cocktail (Roche, Switzerland) and 1% phosphorylase inhibitor cocktail (Roche, Switzerland). The protein concentrations of each sample were determined using a BCA protein assay kit (Beyotime, Jiangsu, China). The samples were separated by 10% SDS gels and were electrophoretically transferred onto polyvinylidene fluoride membranes (PVDF, 0.22 μm, Millipore, USA) with a semidry blotting system (BIO-RAD, USA). After blocking with 5% skim milk for 2 h, the membranes were incubated with the primary antibodies (1:1000) overnight at 4 °C. After washing, the membranes were incubated with horseradish peroxidase (HRP)-conjugated secondary antibody (1:1000, Proteintech Group, China) for 1 h. An enhanced chemiluminescent substrate (ECL) was used to visualize the bands (Fusion Fx5, China) after washing the membranes. The results were evaluated with the gel image analysis software ImageJ 2.1.4.7.

2.7. Statistical analysis

All data are presented as the means ± the SEMs. Before the

statistical analyses, the normality and homogeneity of equal variance were confirmed. One-way ANOVA with Fisher's least-significant differences or two-way repeated ANOVA with multivariate analysis were used to test for differences in treatment groups. The statistical analyses were performed with IBM SPSS Statistics 20.0. $P < .05$ was considered statistically significant.

3. Results

3.1. METH alone has no effect on IL-6 and TNF-α production in microglia

We chose LPS as the inflammatory stimulant because it had been demonstrated to effectively activate microglial cells [37]. To exclude the cytotoxicity of LPS on the microglial cells, LPS dose–response curves were constructed for the BV-2 cells and the primary microglia (10, 100, 500, 1000, and 2000 ng/ml). As illustrated in Supplementary Fig. 1, none of these LPS concentrations elicited overt toxic effects on the cells according to MTT assays (Supplementary Fig. 1a, d). The productions of IL-6 and TNF-α by these two cell types increased in dose-dependent manners and peaked at 1000 and 2000 ng/ml (Supplementary Fig. 1b, c, e, f). Moreover, there were no significant differences in IL-6 or TNF-α activation levels between the 1000 and 2000 ng/ml doses. Thus, we chose the 1000 ng/ml as the dosage to activate the cells.

Based on *in vitro* studies, METH has been demonstrated to influence both humoral and cellular immune responses and to interfere with the normal central immune response [38–40]. Previously, we observed that METH influences murine mast cells [41]. Therefore, we investigated whether METH administration could directly affect microglial cells. Due to the significant toxicity of METH, it was important to establish a sublethal dose that could be used to treat the cells. We constructed dose–response curves (20 μM, 100 μM, 200 μM, and 400 μM) then performed MTT assays on both the BV-2 cells and the primary microglial cells. The cell viabilities, which are presented as the OD values, were significantly inhibited by METH at 400 μM in the BV-2 cells (Supplementary Fig. 2a). The same results were found in the primary microglial cells (Supplementary Fig. 2d). Thus, we used METH at doses < 400 μM in all of the subsequent experiments. When exposed to METH alone and
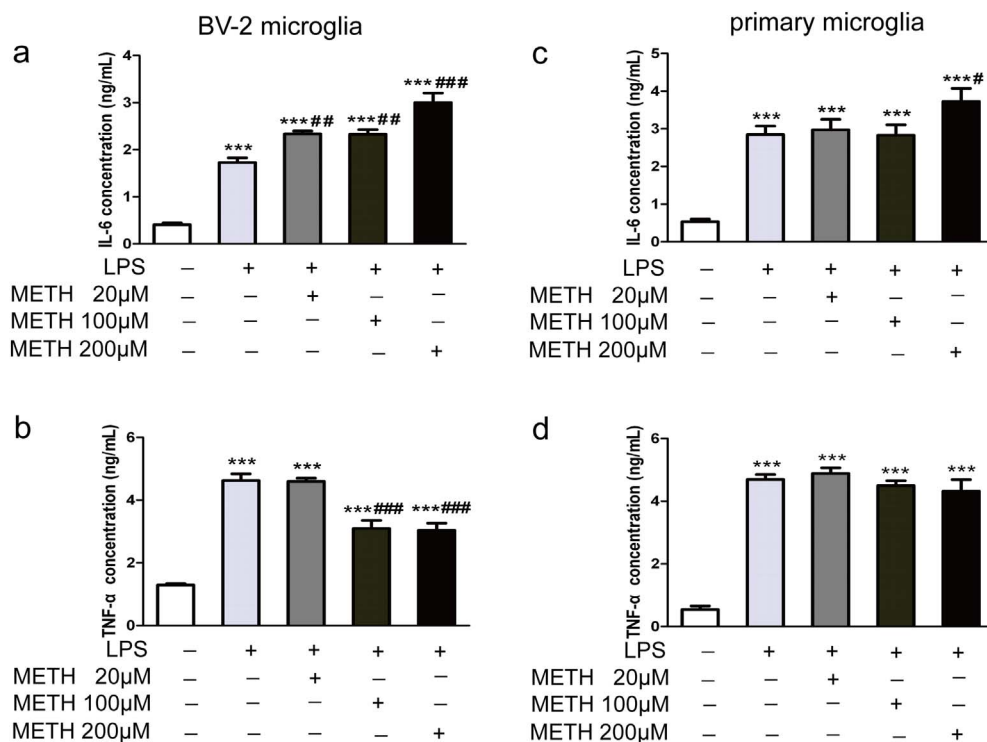
Fig. 2. METH modulates the productions of IL-6 and TNF-α in LPS-activated microglia
BV-2 cells (a, b) and primary microglia (c, d) were incubated with LPS (1 μg/ml) and METH at 20 μM, 100 μM, or 200 μM for 24 h. Then, the supernatants were collected to detect the productions of IL-6 and TNF-α. The data are represented as the means ± the SEMs of three independent experiments, n = 5–6. The statistical analyses were performed using one-way ANOVA and Fisher's LSD test. ***, p < .001, compared to the group without LPS or METH. #, p < .05, ##, p < .01, ###, p < .001, compared to the LPS group.

compared to the control group, the BV-2 cells exhibited no differences in the productions of IL-6 or TNF-α, while LPS significantly increased the productions of these cytokines (Fig. 1a, b). The primary microglial cells also exhibited the same results (Fig. 1c, d). To confirm these findings, we also detected the mRNA of these cytokines and found no differences after METH exposure (Supplementary Fig. 2b, c, e, f).

3.2. METH modulates the productions of IL-6 and TNF-α in LPS-activated microglia

As METH alone did not exhibit regulatory functions on either IL-6 or TNF-α production in resting microglial cells, we were curious whether the results would differ in activated microglial cells. To measure the inflammatory effect of METH exposure on LPS-activated microglial cells, supernatants from all groups of cells were collected, and the IL-6 and TNF-α productions were examined by ELISA assay. After the treatment with METH, the secretion of IL-6 in LPS-activated BV-2 cells was significantly enhanced in a METH-dependent manner, which was most remarkable at the 200-μM dose (Fig. 2a). However, when compared to the LPS group, METH exposure significantly inhibited the production of TNF-α in the LPS-activated BV-2 cells at 100 μM and 200 μM (Fig. 2b). To confirm above changes, we measured the IL-6 and TNF-α production again in primary microglial cells. We found that only the 200-μM dose METH treatment significantly augmented the LPS-induced IL-6 increment in the primary microglial cells when compared to the LPS group (Fig. 2c). However, at the same time, the levels of TNF-α exhibited no difference (Fig. 2d). To exclude the possibility that the regulatory role of METH was due to the excessive or withering cell viability induced by the combined effect of METH and LPS, a regimen of drug combinations was applied to perform an MTT assay. As illustrated in Supplementary Fig. 3, there was no significant difference between the LPS group and the METH + LPS group with respect to the viability of the cells (Supplementary Fig. 3a, d). Moreover, we found that the IL-6 mRNA levels were significantly increased in both the BV-2 cells and the primary microglial cells, while there were no significant changes in TNF-α mRNA production (Supplementary Fig. 3b–c, e-f).

3.3. Effects of METH on the IL-6 and TNF-α time courses in LPS-activated BV-2 cells

To confirm the above results, we designed an experiment that lasted over time course of 24 h to examine the temporal variation characteristics of IL-6 and TNF-α production. We collected supernatants of BV-2 cells at 0.5, 2, 4, 6, 12, and 24 h after LPS challenge to measure the METH-induced alterations in the production of TNF-α and IL-6. Compared to the LPS group, METH significantly increased IL-6 production after 4 h of LPS challenge (Fig. 3a), while METH-mediated TNF-α production decreased earlier after 2 h of LPS treatment (Fig. 3b).

3.4. METH inhibits LPS-induced MAPKs phosphorylation in BV-2 cells, while METH alone had no effect

The MAPK signaling pathways are downstream of TLR4, which is the primary target of LPS and is crucial for the generation of inflammatory cytokines, such as TNF-α and IL-6 [20]. Moreover, three MAPK signaling proteins (ERK1/2, p38 and JNK) tend to differentially affect cytokines, and ERK1/2 has been proven to be fatal for the synthesis, maturity and secretion of TNF-α, while p38 tends to increase the production of IL-1β, IL-6 and JNK regulate nitric oxide [18–22]. As such, we hypothesized that the differential regulation of IL-6 and TNF-α might be triggered by the disparate influences of METH on MAPKs. Because METH exhibited its regulatory effects on the production of IL-6 and TNF-α at doses of 100 μM and 200 μM in the BV-2 cells, it was necessary to detect whether METH regulated MAPK phosphorylations at these doses. We examined the phosphorylation levels of MAPKs after BV-2 cells were incubated with METH for 30 min. As illustrated, METH did not influence the phosphorylation levels of ERK1/2, p38 or JNK when compared to the control group (Fig. 4a-c). However, when the cells were pre-treated with METH, the LPS-induced phosphorylation levels of all the three MAPKs were significantly down-regulated compared to the LPS group (Fig. 4d-f).
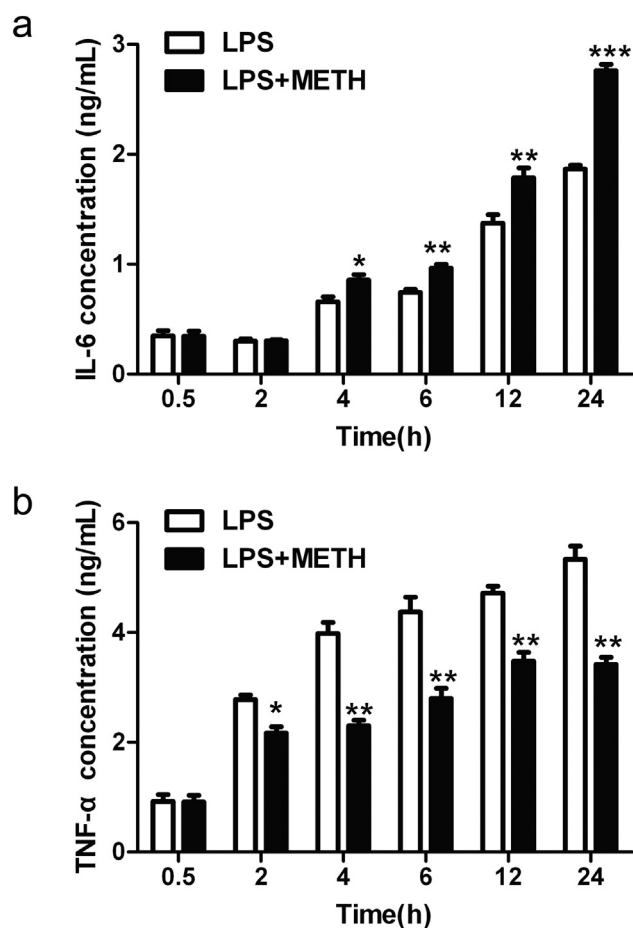
a

b

Fig. 3. Effect of METH on IL-6 and TNF-α time courses in LPS-activated BV-2 cells BV-2 cells were incubated with LPS (1 μg/ml) and METH (200 μM) for 0.5, 2, 4, 6, 12, or 24 h. Next, the supernatants were collected to test the concentrations of IL-6 (a) and TNF-α (b). The data are represented as the means ± the SEMs of three independent experiments, n = 5–6. The statistical analyses were performed using two-way repeated ANOVA followed by multivariate analysis. *, p < .05, **, p < .01, ***, p < .001, compared to the LPS group.

3.5. cAMP/PKA/CREB signaling pathway mediates the regulatory role of METH on IL-6 and TNF-α production in LPS-activated microglial cells

The down-regulated phosphorylation levels of MAPKs mediated by METH, especially that of ERK1/2, could explain the decline in LPS-induced TNF-α production but were contrary to the increment of IL-6. Thus, it was reasonable to guess that another signaling pathway in LPS-activated microglial cells may also be regulated by METH. Other than MAPK signaling, METH has been reported to promote the accumulation of cAMP in astrocytes [32]. It is also known that, as an important second messenger, cAMP can act as an immunoregulatory factor that affects the production of cytokines, including IL-6 [42–45]. Thus, we speculated that the effects of METH on LPS-activated microglial cells might also be mediated by cAMP signaling. We first detected the alterations of cAMP content and the phosphorylation level of CREB, which is the downstream molecule in the cAMP signaling pathway, after the exposure to METH and the LPS challenge in BV-2 cells. As illustrated in Fig. 5, the cAMP concentration was significantly elevated in the METH + LPS group when compared to the LPS group (Fig. 5a). Moreover, the CREB phosphorylation level was also significantly increased by METH in the LPS condition (Fig. 5b). To further determine how cAMP/CREB signaling was involved, we used forskolin, the agonist of the synthetase of cAMP-adenylate cyclase (AC) in LPS-activated BV-2 cells, to test the alterations of IL-6 and TNF-α. As displayed in Fig. 5, forskolin significantly facilitated IL-6 induction but inhibited the

accumulation of TNF-α in the BV-2 cells, which precisely mirrors the actions of METH (Fig. 5c, d). We then used MDL-12330 A, the inhibitor of AC, to measure the changes in cytokines. As illustrated, the METH-induced up-regulation of IL-6 was significantly inhibited by MDL-12330 A (Fig. 5e). The down-regulation of TNF-α by METH was also obviously reversed (Fig. 5f). Considering that the cAMP/PKA/CREB axis is an integral signaling pathway and plays an important role in the immunoregulatory functions of many types of cells [35], PKA may also participate in the above results induced by METH exposure. Thus, we used an inhibitor of PKA, H89, to measure the changes in IL-6 and TNF-α production again. Consequently, H89 pretreatment also distinctly inhibited the METH-mediated up-regulation of IL-6 and reversed the inhibition of TNF-α in LPS-activated BV-2 cells (Fig. 5g, h).

To test the veracity of the results observed in the BV-2 cells, we repeated the experiments in the primary microglial cells. As presented in Fig. 6, the cAMP content and CREB phosphorylation level were both significantly elevated by METH in the LPS condition (Fig. 6a, b). Analogously, MDL-12330 A and H89 reversed the up-regulation of IL-6 in this process (Fig. 6c, e). These inhibitors also exhibited a tendency to promote TNF-α production, whereas METH induced a tendency toward a decrease in TNF-α in the LPS-activated primary microglial cells (Fig. 6d, f).

3.6. Inhibition of the cAMP/PKA/CREB signaling pathway rescues the phosphorylation level of ERK1/2

The above results indicated that the activation of the cAMP/PKA/CREB signaling pathway played a substantial role in METH-induced immunoregulatory function. However, simultaneously, ERK1/2, which is crucial for TNF-α production, is repressed by METH in LPS-activated microglial cells. It has been reported that cAMP and PKA can inhibit or promote the activation of ERK1/2 according to different conditions [46–49]. Therefore, it is important to test whether the down-regulation of phosphorylated ERK1/2 is induced by the activation of cAMP/PKA/CREB signaling. We measured the phosphorylation level of ERK1/2 after the inhibition of cAMP and PKA in both LPS-activated BV-2 cells and primary microglia. As presented, in the BV-2 cells, H89 and MDL-12330 A restored the phosphorylation of ERK1/2 when compared to the METH + LPS group (Fig. 7a, b). Similarly, H89 also significantly rescued ERK1/2 phosphorylation in the primary microglia, while MDL-12330 A only exhibited a recuperative tendency (Fig. 7c, d).

4. Discussion

Ample evidence indicates that METH causes aberrant immune response in microglia and the secretion of pro-inflammatory molecules that leads to neural injury in vivo [50]. However, limited studies have performed on the mechanisms. In this study, the production of IL-6 or TNF-α protein in BV-2 cells and primary microglial cells did not exhibit significantly modulation when they were treated by METH alone, which is consistent with previous study. Frank et al. showed that both the mRNA production of IL-6 and TNF-α in primary microglial cells exhibited no changes when the cells were exposed to METH directly at various doses though the cytokines were up-regulated in vivo [51]. However, we found that METH augmented IL-6 production but inhibited TNF-α production in LPS-activated BV-2 cells. Similarly, METH increased IL-6 production in LPS-induced primary microglial cells but elicited no significant effect on TNF-α production. There is heterogeneity in microglial cells from different sources and they have been proved to exhibit distinct secretion features in inflammatory cytokines when challenged by stimulants [52–55]. For example, when exposed to LPS, primary microglia exhibit high levels of expression and release of TNF-α and IL-6, whereas HAPI microglial cells, a cell line made from rat, exhibit no changes [52]. Thus, the differences in TNF-α production between BV-2 cells and primary microglial cells we found may be due to the different characteristics in the two types of cells. The interesting
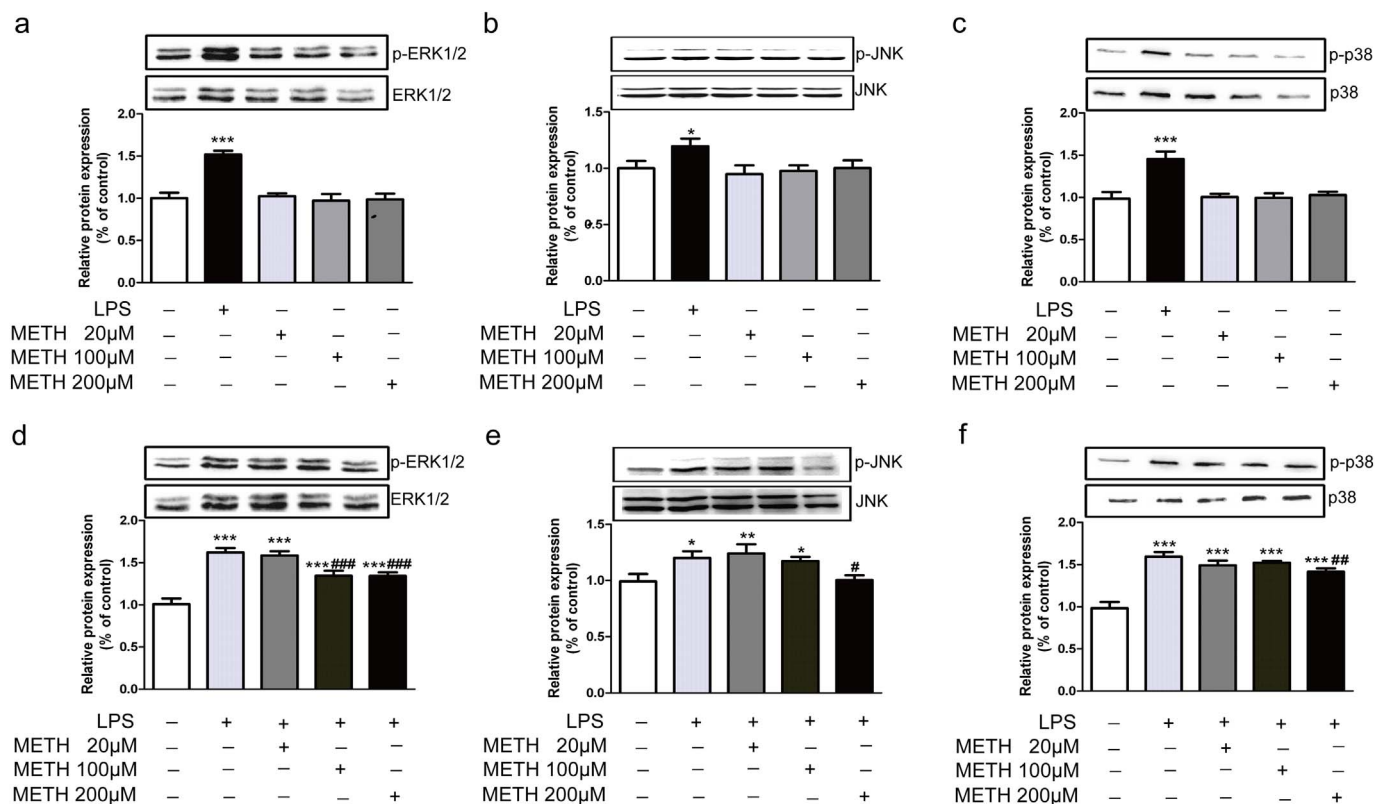
Fig. 4. METH inhibits LPS-induced MAPK phosphorylations in BV-2 cells, while METH alone has no effect

BV-2 cells were incubated with METH at 20 μM, 100 μM, or 200 μM with or without LPS (1 μg/ml) (a-c and d-f respectively) for 30 min. Next, the cells were extracted to assess the phosphorylation levels of ERK1/2, JNK and p38. The data are represented as the means ± the SEMs of three independent experiments. The statistical analyses were performed using one-way ANOVA and Fisher's LSD test. *, $p < .05$, **, $p < .01$, ***, $p < .001$, compared to the group without LPS or METH. #, $p < .05$, ##, $p < .01$, ###, $p < .001$, compared to the LPS group.
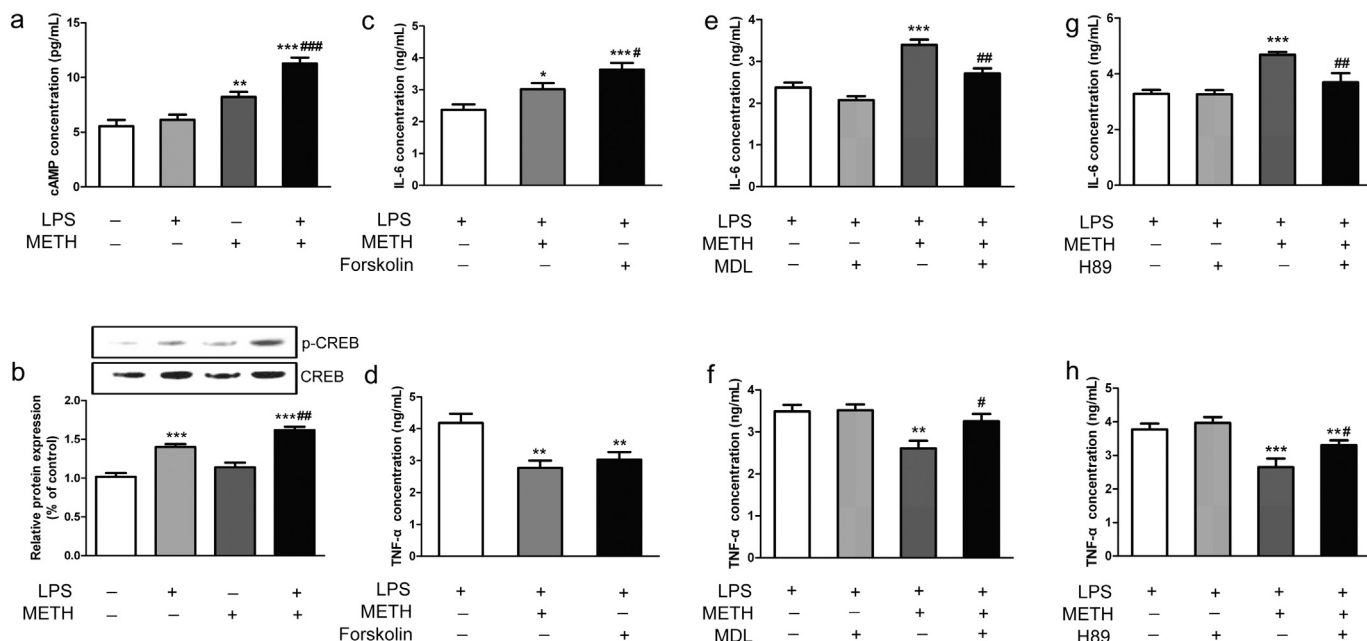

Fig. 5. cAMP/PKA/CREB signaling pathway mediates the regulatory role of METH on IL-6 and TNF-α production in LPS-activated BV-2 cells.

(a) BV-2 cells were incubated with METH (200 μM) and LPS (1 μg/ml) for 15 min. Next, the cell extracts were collected and tested for the concentration of cAMP. (b) BV-2 cells were incubated with METH and LPS for 30 min then were extracted to assess the phosphorylation of CREB. Forskolin (10 μM) (c, d), MDL-12330A (10 μM) (e, f) and H89 (30 μM) (g, h) were added with METH and LPS for 24 h. After that step, the supernatants were measured for IL-6 and TNF-α production. The data are represented as the means ± the SEMs of three independent experiments, n = 5–6. The statistical analyses were performed using one-way ANOVA and Fisher's LSD test. *, $p < .05$, **, $p < .01$, ***, $p < .001$, compared to the group without LPS and METH (a, b) or the LPS group (c-h). #, $p < .05$, ##, $p < .01$, ###, $p < .001$, compared to the LPS group (a, b), METH group (c, d) or LPS + METH group (e-h).
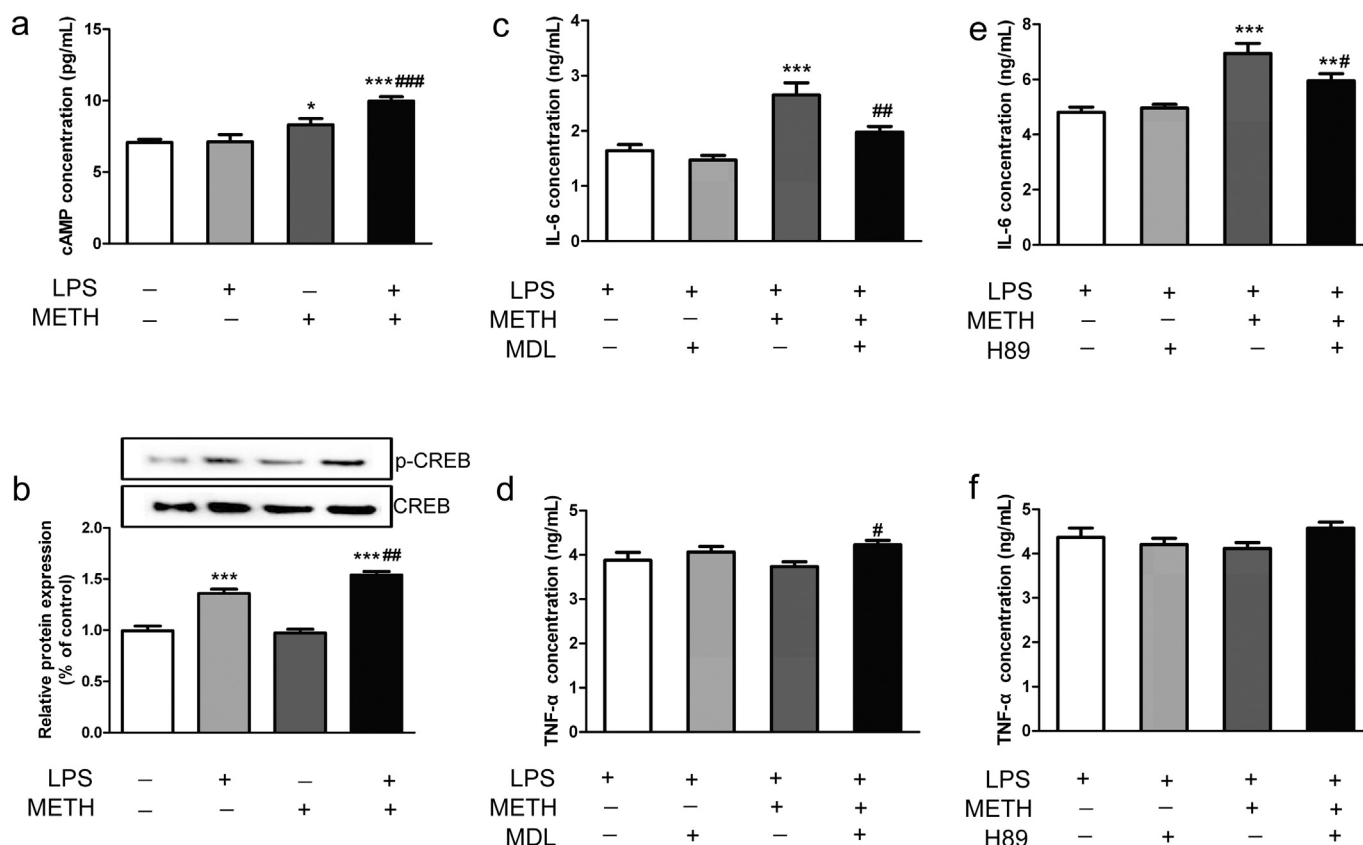
Fig. 6. cAMP/PKA/CREB signaling pathway mediates the regulatory role of METH on IL-6 and TNF-α production in LPS-activated primary microglia
(a) Primary microglia were incubated with METH (200 μM) and LPS (1 μg/ml) for 15 min. After that step, the cell extracts were collected and tested for the concentration of cAMP. (b) Primary microglia were incubated with METH and LPS for 30 min and were then extracted to assess the phosphorylation of CREB. MDL-12330A (10 μM) (c, d) and H89 (30 μM) (e, f) were added with METH and LPS for 24 h. Next, the supernatants were measured for IL-6 and TNF-α production. The data are represented as the means ± the SEMs of three independent experiments, n = 5–6. The statistical analyses were performed using one-way ANOVA and Fisher's LSD test. *, p < .05, **, p < .01, ***, p < .001, compared to the group without LPS and METH (a, b) or the LPS group(c-f). #, p < .05, ##, p < .01, ###, p < .001, compared to the LPS group (a, b) or the LPS + METH group (c-f).

aspect of this result was that METH exhibited different regulatory roles on IL-6 and TNF-α in LPS-activated microglial cells. Our previous study in Raw264.7 macrophages also showed different outcomes in IL-6 and TNF-α (data not shown). However these were contrary to Coelho-Santos's e report that both IL-6 and TNF-α increased when N9 microglial cells were incubated with increasing concentrations (0.1, 0.5, 1, 2 and 4 mM) of METH [56]. This difference may be primarily due to two reasons. First, the N9 cell line was used in their experiments, and this cell line exhibits great differences from BV-2 cells and primary microglia [53]. Second, the dose of METH used by these authors reached up to 4000 nM, i.e., a dose that induces significant cell death and then triggers high levels of cell activation due to the cell debris [57]. Furthermore, divergent regulation of IL-6 and TNF-α in a single cell type has also been reported, for example, cholera toxin, which increases intracellular cAMP, concomitantly increases IL-6 synthesis but decreases TNF-α production in rat peritoneal mast cells [25]. Nevertheless, above results suggest that METH can differently modulate the production of the cytokines IL-6 and TNF-α in LPS-activated microglial cells and cAMP may be involved in that process.

It is widely accepted that IL-6 has the ability to affect the production of TNF-α [25,58]. Thus, we wondered whether the decrement of TNF-α was due to the elevated IL-6 in BV-2 cells. We examined the production of IL-6 and TNF-α during 24 h in LPS-activated BV-2 cells in response to METH. We found that IL-6 was increased at 4, 6, 12, and 24 h, while TNF-α was inhibited at 2, 4, 6, 12, and 24 h after the pretreatment of METH on LPS-activated BV-2 cells. In other words, the decrement of TNF-α occurred earlier than the increment of IL-6 and this might hint us that IL-6 did not inhibit the TNF-α production in our experiments though this need more evidences. According to previous reports, the

inhibitory role of IL-6 on TNF-α may require the help of other molecules, such as the pituitary adenylate cyclase-activating polypeptide (PACAP) type receptor, which can be activated by maxadilan and then induce a negative-feedback mechanism that controls certain inflammatory responses [59–62]. These molecules, such as PACAP, might not exist in microglial cells and further research is required to prove this.

LPS simultaneously increases IL-6 synthesis and TNF-α production mainly via LBP-CD4/TLR4/MyD88/MAPK [25,63]. Thus, the changes in the phosphorylation levels of p38, JNK and ERK1/2 were observed in our study. We found that LPS significantly increased their phosphorylation levels while METH alone showed no effect. We also found that METH pretreatment reduced the LPS-induced phosphorylation levels of all the three molecules-p38, JNK and ERK1/2. This down-regulation of MAPKs was in agreement with the inhibition on TNF-α by METH, but was contrary to the increment of IL-6, suggesting another mechanism may be involved in.

It's commonly known that CREB is one of the regulative signaling proteins which are responsible for inflammatory cytokines, such as IL-6 [64]. CREB is also the classic target molecule in response to METH. It can mediate METH-induced spatial memory consolidation, retrieval and reconsolidation [65]. In addition, CREB is regulated by METH as a part of cAMP/PKA/CREB signaling pathway both in vivo and in vitro [66,67]. In the present study, we also found that forskolin, an agonist of cAMP, elevated the LPS-induced IL-6 production while inhibited TNF-α. In addition, when compared to LPS group, we found that simultaneous exposure to METH significantly promoted the cAMP content and CREB phosphorylation levels. This indicated the involvement of cAMP/PKA/CREB signaling pathway. To verify this further, we used the AC
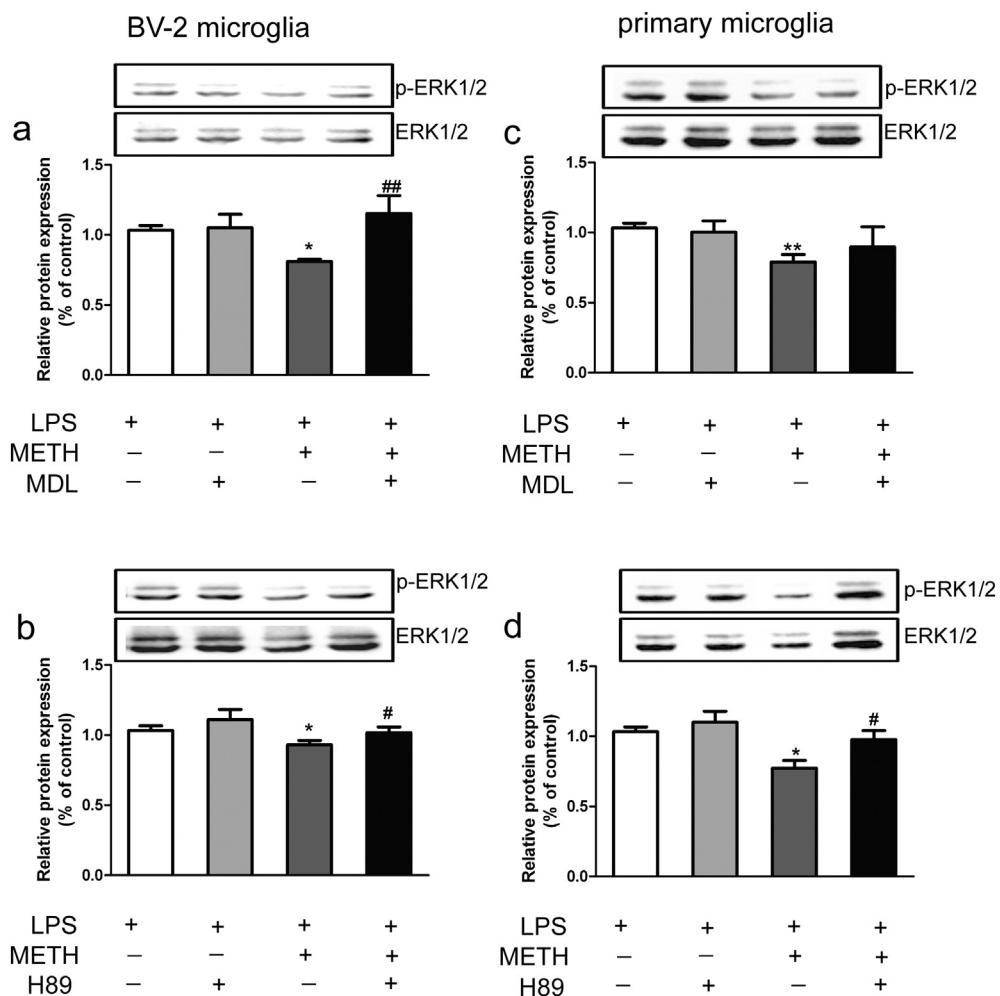
BV-2 microglia

a

primary microglia

c

b

d

Fig. 7. Inhibition of cAMP/PKA/CREB signaling pathway rescues the phosphorylation level of ERK1/2

(a, c) Microglial cells were incubated with MDL-12330A (10 μM) and LPS or METH for 30 min to measure the phosphorylation of ERK1/2. (b, d) Microglial cells were incubated with H89 (30 μM) and LPS or METH to measure the phosphorylation of ERK1/2. The data are represented as the means ± the SEMs of three independent experiments. The statistical analyses were performed using one-way ANOVA and Fisher's LSD test. *, $p < .05$, **, $p < .01$, compared to the LPS group, #, $p < .05$, ##, $p < .01$, compared to the LPS + METH group.

inhibitor MDL-12, 330A to inhibit the cAMP and it inhibited the METH-induced up-regulation of IL-6 and rescued the production of TNF-α at the same time. Moreover, we also used the PKA inhibitor H89, which also reversed the METH-induced regulation on IL-6 and TNF-α. These results confirmed the participation of the cAMP/PKA/CREB axis. In airway smooth muscle cells and human chondrocytes, the involvement of cAMP/PKA/CREB axis in IL-6 and TNF-α regulation has been discovered [34,68]. In addition, the axis was also reported to regulate cytokines production in many other cell types, such as Caco-2 cells, mononuclear cells and cardiac fibroblasts [44,45,48,69]. Therefore, we speculated that the METH-induced modulations on the productions of IL-6 and TNF-α in LPS-activated microglial cells are mediated by the cAMP/PKA/CREB signaling pathway. As to the significant role of cAMP, a receptor coupled to protein Gs would be a plausible intermediate. *In vivo*, METH works mainly through the activation of dopamine receptors (DRs) among which D1DR and D5DR are protein Gs-coupled [70]. In view of this, we also used their agonists dopamine and SKF 38393 as well as the antagonist SCH 23390 to detect their possible role. But as a pity, they showed no effect on the production of IL-6 and TNF-α (data not shown). So, whether the effect of METH on microglia was receptor-mediated need more evidence which may be found on other receptors and we will focus on this in the following work.

In our results, MAPKs were inhibited while the cAMP/PKA/CREB signaling pathway was activated by METH in LPS-activated microglial cells. It seemed to be a paradox. In the MAPKs, ERK1/2 is crucial to the TNF-α production by promoting the localization of pre-TNF-α to the cell surface [71,72]. To answer the question why the production of TNF-α was decremented in LPS-activated microglial cells in response to

METH, ERK1/2 was chosen as the key study object in MAPKs. In some conditions, cAMP/PKA/CREB signaling pathway shows suppressant effect on ERK1/2 [73,74]. Thus, the phosphorylation levels of ERK1/2 were determined after MDL-12, H89 administration. We found MDL-12, 330A induced the rescue of ERK1/2 phosphorylation when it was given before METH and LPS. H89 treatment also exhibited the same results. In monocytes, PKA is also reported to induce the suppression of TNF-α production by inhibition on Raf-1, which is the upstream of ERK1/2 [75]. These results proved that the diminished phosphorylation level of ERK1/2 by METH was due to the activation of the cAMP/PKA/CREB signaling pathway (Fig. 8). The inhibition on ERK1/2 by cAMP/PKA signaling was also reported in vascular smooth muscle cells that it suppresses the proliferation of the cells [73]. As summarized in Fig. 8, these results indicated the existence of crosstalk between cAMP/PKA/CREB and LPS/ERK1/2 in LPS-activated microglial cells at ERK1/2 phosphorylation inhibited by CREB. However, LPS shows the limited possibility to challenge all the METH users excepting those who are infected by Gram-negative bacteria while amyloid β-protein and cytokines, such as INF-γ, are more commonly seen in the brain [16,17]. Thus, it's necessary to detect the regulatory role of METH on microglial immune response to the above stimuli in the following work. Nevertheless, the study reported here hinted us at the various mechanisms underline the immune impacts induced by METH.

5. Conclusions

Taken together, our results demonstrate that METH can differently modulate the production of the cytokines IL-6 and TNF-α in LPS-
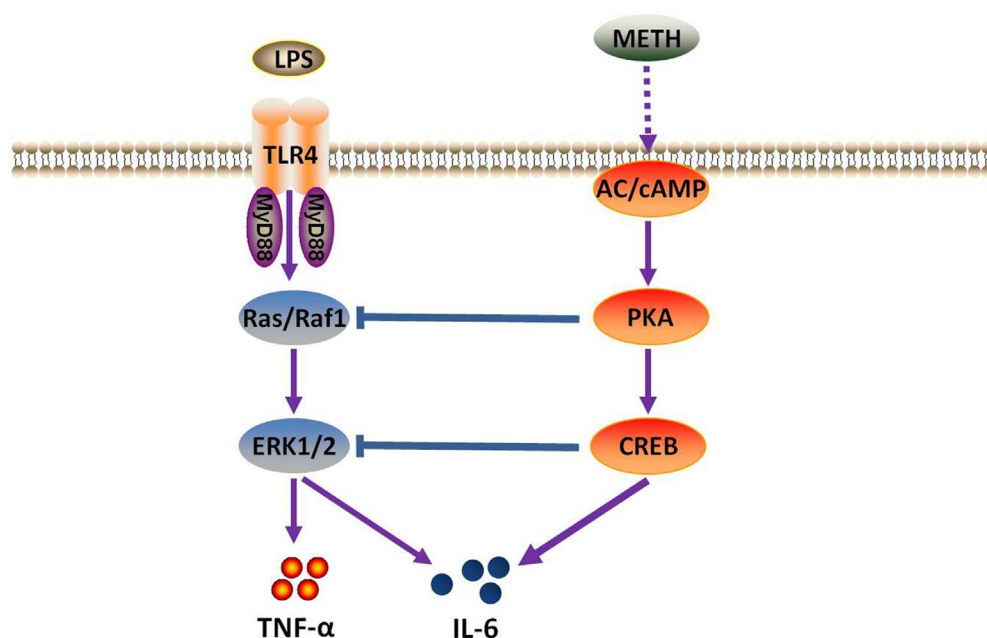
Fig. 8. The proposed mechanism underlying METH-induced immune modulation in LPS-activated microglial cells.
LPS binds to TLR4 on the surface of microglial cells, and activates Ras/Raf1 and ERK1/2 to up-regulate the production of IL-6 and TNF-α. When exposed to METH, the activation of AC is triggered and it induces high expression level of cAMP, activates PKA and promotes the phosphorylation of CREB. The activation of cAMP/PKA/CREB signaling pathway up-regulates IL-6 production while resulting in the inhibition of ERK1/2-mediated TNF-α expression.

activated microglial cells. The cAMP/PKA/CREB signaling pathway mediates this modulation. Our study provides insight into the immunoregulatory activity of METH on activated microglia, and indicates that the cAMP/PKA/CREB signaling pathway may be a potential target for remedying METH relevant neuroinflammation and neurotoxicity.

Abbreviations

METH   methamphetamine
IL-6   interleukin-6
TNF-α   tumor necrosis factor-α
cAMP   cyclic adenosine monophosphate
ERK1/2   extracellular regulated kinase1/2
JNK   c-Jun N-terminal kinase
PKA   protein kinase A
CREB   cAMP-response element binding protein;
MTT   3-(4,5-dimethylthiazol-2-yl)-2,5-diphenyltetra-zolium bromide

Acknowledgments

Appendix A. Supplementary data

Supplementary data to this article can be found online at https://doi.org/10.1016/j.intimp.2018.01.024.

References

[1] M.D. Anglin, C. Burke, B. Perrochet, E. Stamper, S. Dawud-Noursi, History of the methamphetamine problem, J. Psychoactive Drugs 32 (2) (2000) 137–141.
[2] T.E. Freese, K. Miotto, C.J. Reback, The effects and consequences of selected club drugs, J. Subst. Abus. Treat. 23 (2) (2002) 151–156.
[3] H. Friedman, S. Pross, T.W. Klein, Addictive drugs and their relationship with infectious diseases, FEMS Immunol. Med. Microbiol. 47 (3) (2006) 330–342.
[4] J.B. Buchanan, N.L. Sparkman, R.W. Johnson, A neurotoxic regimen of methamphetamine exacerbates the febrile and neuroinflammatory response to a subsequent peripheral immune stimulus, J. Neuroinflammation 7 (2010) 82.
[5] N. Atallah, R. Vasiu, A.B. Bosca, D.I. Cretu, C. Georgiu, A.M. Constantin, A.S. Sovrea, Microglia–performers of the 21st century, Romanian J. Morphol. Embryol. 55 (3) (2014) 745–765.
[6] N.C. Fernandes, U. Sriram, L. Gofman, J.M. Cenna, S.H. Ramirez, R. Potula, Methamphetamine alters microglial immune function through P2X7R signaling, J. Neuroinflammation 13 (1) (2016) 91.
[7] M.E. Lull, M.L. Block, Microglial activation and chronic neurodegeneration, Neurotherapeutics 7 (4) (2010) 354–365.
[8] G.W. Kreutzberg, Microglia: a sensor for pathological events in the CNS, Trends Neurosci. 19 (8) (1996) 312–318.
[9] A. Jucaite, P. Svenningsson, J.O. Rinne, Z. Cselenyi, K. Varnas, P. Johnstrom, N. Amini, A. Kirjavainen, S. Helin, M. Minkwitz, A.R. Kugler, J.A. Posener, S. Budd, C. Halldin, A. Varrone, L. Farde, Effect of the myeloperoxidase inhibitor AZD3241 on microglia: a PET study in Parkinson's disease, Brain 138 (Pt 9) (2015) 2687–2700.
[10] A. Gerhard, N. Pavese, G. Hotton, F. Turkheimer, M. Es, A. Hammers, K. Eggert, W. Oertel, R.B. Banati, D.J. Brooks, In vivo imaging of microglial activation with [11C](R)-PK11195 PET in idiopathic Parkinson's disease, Neurobiol. Dis. 21 (2) (2006) 404–412.
[11] D.M. Thomas, D.M. Kuhn, Attenuated microglial activation mediates tolerance to the neurotoxic effects of methamphetamine, J. Neurochem. 92 (4) (2005) 790–797.
[12] D.M. Thomas, D.M. Kuhn, MK-801 and dextromethorphan block microglial activation and protect against methamphetamine-induced neurotoxicity, Brain Res. 1050 (1–2) (2005) 190–198.
[13] J. Goncalves, S. Baptista, T. Martins, N. Milhazes, F. Borges, C.F. Ribeiro, J.O. Malva, A.P. Silva, Methamphetamine-induced neuroinflammation and neuronal dysfunction in the mice hippocampus: preventive effect of indomethacin, Eur. J. Neurosci. 31 (2) (2010) 315–326.
[14] E. Xu, J. Liu, H. Liu, X. Wang, H. Xiong, Role of microglia in methamphetamine-induced neurotoxicity, Int. J. Physiol. Pathophysiol. Pharmacol. 9 (3) (2017) 84–100.
[15] V. Bocchini, R. Mazzolla, R. Barluzzi, E. Blasi, P. Sick, H. Kettenmann, An immortalized cell line expresses properties of activated microglial cells, J. Neurosci. Res. 31 (4) (1992) 616–621.
[16] K.U. Tufekci, R. Meuwissen, S. Genc, K. Genc, Inflammation in Parkinson's disease,

Adv. Protein Chem. Struct. Biol. 88 (2012) 69–132.

[17] T.M. Weitz, T. Town, Microglia in Alzheimer's disease: it's all about context, Int. J. Alzheimers Dis. 2012 (2012) 314185.

[18] D.O. Moon, Y.H. Choi, N.D. Kim, Y.M. Park, G.Y. Kim, Anti-inflammatory effects of beta-lapachone in lipopolysaccharide-stimulated BV2 microglia, Int. Immunopharmacol. 7 (4) (2007) 506–514.

[19] Y.T. Yeung, N.S. Bryce, S. Adams, N. Braidy, M. Konayagi, K.L. McDonald, C. Teo, G.J. Guillemin, T. Grewal, L. Munoz, p38 MAPK inhibitors attenuate pro-in-flammatory cytokine production and the invasiveness of human U251 glioblastoma cells, J. Neuro-Oncol. 109 (1) (2012) 35–44.

[20] T. Pang, J. Wang, J. Benicky, E. Sanchez-Lemus, J.M. Saavedra, Telmisartan directly ameliorates the neuronal inflammatory response to IL-1beta partly through the JNK/c-Jun and NADPH oxidase pathways, J. Neuroinflammation 9 (2012) 102.

[21] S. Rousseau, M. Papoutsopoulou, A. Symons, D. Cook, J.M. Lucocq, A.R. Prescott, A. O'Garra, S.C. Ley, P. Cohen, TPL2-mediated activation of ERK1 and ERK2 reg-ulates the processing of pre-TNF alpha in LPS-stimulated macrophages, J. Cell Sci. 121 (Pt 2) (2008) 149–154.

[22] X. Shao, Y. Qin, H. Wang, Y. Gao, C. Cheng, A. Shen, The role of ERK in LPS induced TNF-alpha expression on Schwann cells, Chin. J. Microbiol. Immunol. (2007) 485–489.

[23] J.Y. Lo, M.N. Kamarudin, O.A. Hamdi, K. Awang, H.A. Kadir, Curcumenol isolated from *Curcuma zedoaria* suppresses Akt-mediated NF-kappaB activation and p38 MAPK signaling pathway in LPS-stimulated BV-2 microglial cells, Food Funct. 6 (11) (2015) 3550–3559.

[24] L. Li, J. Lu, S.S. Tay, S.M. Moochhala, B.P. He, The function of microglia, either neuroprotection or neurotoxicity, is determined by the equilibrium among factors released from activated microglia in vitro, Brain Res. 1159 (2007) 8–17.

[25] I. Leal-Berumen, D.P. Snider, C. Barajas-Lopez, J.S. Marshall, Cholera toxin in-creases IL-6 synthesis and decreases TNF-alpha production by rat peritoneal mast cells, J. Immunol. 156 (1) (1996) 316–321.

[26] S. Ding, W. Wang, X. Wang, Y. Liang, L. Liu, Y. Ye, J. Yang, H. Gao, Q. Zhuge, Dopamine burden triggers neurodegeneration via production and release of TNF-alpha from astrocytes in minimal hepatic encephalopathy, Mol. Neurobiol. 53 (8) (2016) 5324–5343.

[27] I.A. Clark, B. Vissel, A neurologist's guide to TNF biology and to the principles behind the therapeutic removal of excess TNF in disease, Neural Plast. 2015 (2015) 358263.

[28] E. Tatlidil Yaylaci, R.N. Yuksel, K. Unal, N. Altunsoy, M. Cingi, S. Yalcin Sahiner, M.C. Aydemir, E. Goka, TNF-related weak inducer of apoptosis (TWEAK) levels in schizophrenia, Psychiatry Res. 229 (3) (2015) 755–759.

[29] S. Merighi, S. Gessi, K. Varani, D. Fazzi, P. Mirandola, P.A. Borea, Cannabinoid CB (2) receptor attenuates morphine-induced inflammatory responses in activated microglial cells, Br. J. Pharmacol. 166 (8) (2012) 2371–2385.

[30] C. Wang, L. Deng, M. Hong, G.R. Akkaraju, J. Inoue, Z.J. Chen, TAK1 is a ubiquitin-dependent kinase of MKK and IKK, Nature 412 (6844) (2001) 346–351.

[31] W. Han, Y. Takamatsu, H. Yamamoto, S. Kasai, S. Endo, T. Shirao, N. Kojima, K. Ikeda, Inhibitory role of inducible cAMP early repressor (ICER) in methamphe-tamine-induced locomotor sensitization, PLoS One 6 (6) (2011) e21637.

[32] I.E. Cisneros, A. Ghorpade, Methamphetamine and HIV-1-induced neurotoxicity: role of trace amine associated receptor 1 cAMP signaling in astrocytes, Neuropharmacology 85 (2014) 499–507.

[33] E.M. Mack, J.E. Smith, S.G. Kurz, J.R. Wood, cAMP-dependent regulation of ovu-latory response genes is amplified by IGF1 due to synergistic effects on Akt phos-phorylation and NF-kappaB transcription factors, Reproduction 144 (5) (2012) 595–602.

[34] P. Wang, F. Zhu, K. Konstantopoulos, Prostaglandin E2 induces interleukin-6 ex-pression in human chondrocytes via cAMP/protein kinase A- and phosphatidyli-nositol 3-kinase-dependent NF-kappaB activation, Am. J. Phys. Cell Phys. 298 (6) (2010) C1445–56.

[35] W. Zhao, Y. Huang, Z. Liu, B.B. Cao, Y.P. Peng, Y.H. Qiu, Dopamine receptors modulate cytotoxicity of natural killer cells via cAMP-PKA-CREB signaling pathway, PLoS One 8 (6) (2013) e65860.

[36] C.M. Sondag, C.K. Combs, Amyloid precursor protein cross-linking stimulates beta amyloid production and pro-inflammatory cytokine release in monocytic lineage cells, J. Neurochem. 97 (2) (2006) 449–461.

[37] J.N. Dai, Y. Zong, L.M. Zhong, Y.M. Li, W. Zhang, L.G. Bian, Q.L. Ai, Y.D. Liu, J. Sun, D. Lu, Gastrodin inhibits expression of inducible NO synthase, cyclooxygenase-2 and proinflammatory cytokines in cultured LPS-stimulated microglia via MAPK pathways, PLoS One 6 (7) (2011) e21891.

[38] R.V. House, P.T. Thomas, H.N. Bhargava, Comparison of immune functional para-meters following in vitro exposure to natural and synthetic amphetamines, Immunopharmacol. Immunotoxicol. 16 (1) (1994) 1–21.

[39] M. Iwasa, Y. Maeno, H. Inoue, H. Koyama, R. Matoba, Induction of apoptotic cell death in rat thymus and spleen after a bolus injection of methamphetamine, Int. J. Legal Med. 109 (1) (1996) 23–28.

[40] J.B. Buchanan, N.L. Sparkman, R.W. Johnson, Methamphetamine sensitization at-tenuates the febrile and neuroinflammatory response to a subsequent peripheral immune stimulus, Brain Behav. Immun. 24 (3) (2010) 502–511.

[41] L. Xue, X. Li, H.X. Ren, F. Wu, M. Li, B. Wang, F.Y. Chen, W.Y. Cheng, J.P. Li, Y.J. Chen, T. Chen, The dopamine D3 receptor regulates the effects of metham-phetamine on LPS-induced cytokine production in murine mast cells, Immunobiology 220 (6) (2015) 744–752.

[42] C.A. Isoni, E.A. Borges, C.A. Veloso, R.T. Mattos, M.M. Chaves, J.A. Nogueira-Machado, cAMP activates the generation of reactive oxygen species and inhibits the secretion of IL-6 in peripheral blood mononuclear cells from type 2 diabetic pa-tients, Oxidative Med. Cell. Longev. 2 (5) (2009) 317–321.

[43] R.L. Robson, J. Westwick, Z. Brown, Interleukin-1-induced IL-8 and IL-6 gene ex-pression and production in human mesangial cells is differentially regulated by cAMP, Kidney Int. 48 (6) (1995) 1767–1777.

[44] D.D. Hershko, B.W. Robb, G. Luo, P.O. Hasselgren, Multiple transcription factors regulating the IL-6 gene are activated by cAMP in cultured Caco-2 cells, Am. J. Phys. Regul. Integr. Comp. Phys. 283 (5) (2002) R1140–8.

[45] F. Yin, Y.Y. Wang, J.H. Du, C. Li, Z.Z. Lu, C. Han, Y.Y. Zhang, Noncanonical cAMP pathway and p38 MAPK mediate beta2-adrenergic receptor-induced IL-6 produc-tion in neonatal mouse cardiac fibroblasts, J. Mol. Cell. Cardiol. 40 (3) (2006) 384–393.

[46] C. Hecquet, G. Lefevre, M. Valtink, K. Engelmann, F. Mascarelli, cAMP inhibits the proliferation of retinal pigmented epithelial cells through the inhibition of ERK1/2 in a PKA-independent manner, Oncogene 21 (39) (2002) 6101–6112.

[47] D. Chiluiza, S. Krishna, V.A. Schumacher, J. Schlondorff, Gain-of-function muta-tions in transient receptor potential C6 (TRPC6) activate extracellular signal-regu-lated kinases 1/2 (ERK1/2), J. Biol. Chem. 288 (25) (2013) 18407–18420.

[48] E. Damm, T.R. Buech, T. Gudermann, A. Breit, Melanocortin-induced PKA activa-tion inhibits AMPK activity via ERK-1/2 and LKB-1 in hypothalamic GT1-7 cells, Mol. Endocrinol. 26 (4) (2012) 643–654.

[49] A.J. Murray, Pharmacological PKA inhibition: all may not be what it seems, Sci. Signal. 1 (22) (2008) re4.

[50] D.M. Thomas, P.D. Walker, J.A. Benjamins, T.J. Geddes, D.M. Kuhn, Methamphetamine neurotoxicity in dopamine nerve endings of the striatum is as-sociated with microglial activation, J. Pharmacol. Exp. Ther. 311 (1) (2004) 1–7.

[51] M.G. Frank, S. Adhikary, J.L. Sobesky, M.D. Weber, L.R. Watkins, S.F. Maier, The danger-associated molecular pattern HMGB1 mediates the neuroinflammatory ef-fects of methamphetamine, Brain Behav. Immun. 51 (2016) 99–108.

[52] R.J. Horvath, N. Nutile-McMenemy, M.S. Alkaitis, J.A. Deleo, Differential migra-tion, LPS-induced cytokine, chemokine, and NO expression in immortalized BV-2 and HAPI cell lines and primary microglial cultures, J. Neurochem. 107 (2) (2008) 557–569.

[53] L. Duan, B.Y. Chen, X.L. Sun, Z.J. Luo, Z.R. Rao, J.J. Wang, L.W. Chen, LPS-induced proNGF synthesis and release in the N9 and BV2 microglial cells: a new pathway underling microglial toxicity in neuroinflammation, PLoS One 8 (9) (2013) e73768.

[54] H. Scheiblich, F. Roloff, V. Singh, M. Stangel, M. Stern, G. Bicker, Nitric oxide/cyclic GMP signaling regulates motility of a microglial cell line and primary mi-croglia in vitro, Brain Res. 1564 (2014) 9–21.

[55] A. Henn, S. Lund, M. Hedtjarn, A. Schrattenholz, P. Porzgen, M. Leist, The suit-ability of BV2 cells as alternative model system for primary microglia cultures or for animal experiments examining brain inflammation, ALTEX 26 (2) (2009) 83–94.

[56] V. Coelho-Santos, J. Goncalves, C. Fontes-Ribeiro, A.P. Silva, Prevention of me-thamphetamine-induced microglial cell death by TNF-alpha and IL-6 through ac-tivation of the JAK-STAT pathway, J. Neuroinflammation 9 (2012) 103.

[57] N.P. Restifo, Building better vaccines: how apoptotic cell death can induce in-flammation and activate innate and adaptive immunity, Curr. Opin. Immunol. 12 (5) (2000) 597–603.

[58] D. Aderka, J.M. Le, J. Vilcek, IL-6 inhibits lipopolysaccharide-induced tumor ne-crosis factor production in cultured human monocytes, U937 cells, and in mice, J. Immunol. 143 (11) (1989) 3517–3523.

[59] R. Starkie, S.R. Ostrowski, S. Jauffred, M. Febbraio, B.K. Pedersen, Exercise and IL-6 infusion inhibit endotoxin-induced TNF-alpha production in humans, FASEB J. 17 (8) (2003) 884–886.

[60] A.M. Petersen, B.K. Pedersen, The role of IL-6 in mediating the anti-inflammatory effects of exercise, J. Physiol. Pharmacol. 57 (Suppl. 10) (2006) 43–51.

[61] B.K. Pedersen, A. Steensberg, C. Fischer, C. Keller, P. Keller, P. Plomgaard, M. Febbraio, B. Saltin, Searching for the exercise factor: is IL-6 a candidate? J. Muscle Res. Cell Motil. 24 (2–3) (2003) 113–119.

[62] M.B. Soares, R.G. Titus, C.B. Shoemaker, J.R. David, M. Bozza, The vasoactive peptide maxadilan from sand fly saliva inhibits TNF-alpha and induces IL-6 by mouse macrophages through interaction with the pituitary adenylate cyclase-acti-vating polypeptide (PACAP) receptor, J. Immunol. 160 (4) (1998) 1811–1816.

[63] R. Gorina, M. Font-Nieves, L. Marquez-Kisinousky, T. Santalucia, A.M. Planas, Astrocyte TLR4 activation induces a proinflammatory environment through the interplay between MyD88-dependent NFkappaB signaling, MAPK, and Jak1/Stat1 pathways, Glia 59 (2) (2011) 242–255.

[64] K.R. Chava, M. Karpurapu, D. Wang, M. Bhanoori, V. Kundumani-Sridharan, Q. Zhang, T. Ichiki, W.C. Glasgow, G.N. Rao, CREB-mediated IL-6 expression is required for 15(S)-hydroxyeicosatetraenoic acid-induced vascular smooth muscle cell migration, Arterioscler. Thromb. Vasc. Biol. 29 (6) (2009) 809–815.

[65] G. Cao, J. Zhu, Q. Zhong, C. Shi, Y. Dang, W. Han, X. Liu, M. Xu, T. Chen, Distinct roles of methamphetamine in modulating spatial memory consolidation, retrieval, reconsolidation and the accompanying changes of ERK and CREB activation in hippocampus and prefrontal cortex, Neuropharmacology 67 (2013) 144–154.

[66] Y. Yan, A. Nitta, T. Mizuno, A. Nakajima, K. Yamada, T. Nabeshima, Discriminative-stimulus effects of methamphetamine and morphine in rats are attenuated by cAMP-related compounds, Behav. Brain Res. 173 (1) (2006) 39–46.

[67] M. Levite, Dopamine and T cells: dopamine receptors and potent effects on T cells, dopamine production in T cells, and abnormalities in the dopaminergic system in T cells in autoimmune, neurological and psychiatric diseases, Acta Physiol (Oxford) 216 (1) (2016) 42–89.

[68] A.S. Bogard, A.V. Birg, R.S. Ostrom, Non-raft adenylyl cyclase 2 defines a cAMP signaling compartment that selectively regulates IL-6 expression in airway smooth muscle cells: differential regulation of gene expression by AC isoforms, Naunyn Schmiedeberg's Arch. Pharmacol. 387 (4) (2014) 329–339.

[69] M. Ghosh, Y. Xu, D.D. Pearse, Cyclic AMP is a key regulator of M1 to M2a phe-notypic conversion of microglia in the presence of Th2 cytokines, J.

Neuroinflammation 13 (2016) 9.

[70] P.K. Thanos, R. Kim, F. Delis, M.J. Rocco, J. Cho, N.D. Volkow, Effects of chronic methamphetamine on psychomotor and cognitive functions and dopamine signaling in the brain, Behav. Brain Res. 320 (2017) 282–290.

[71] C.M. Thomas, T. Hong, J.P. van Pijkeren, P. Hemarajata, D.V. Trinh, W. Hu, R.A. Britton, M. Kalkum, J. Versalovic, Histamine derived from probiotic lactobacillus reuteri suppresses TNF via modulation of PKA and ERK signaling, PLoS One 7 (2) (2012) e31951.

[72] J.F. Foley, No TNF-α Secretion Without ERK Activation, Sci. Signal. 1 (2) (2008) ec15.

[73] D. Liu, Y. Huang, D. Bu, A.D. Liu, L. Holmberg, Y. Jia, C. Tang, J. Du, H. Jin, Sulfur dioxide inhibits vascular smooth muscle cell proliferation via suppressing the Erk/MAP kinase pathway mediated by cAMP/PKA signaling, Cell Death Dis. 5 (2014) e1251.

[74] J.L. Maymo, A. Perez Perez, B. Maskin, J.L. Duenas, J.C. Calvo, V. Sanchez Margalet, C.L. Varone, The alternative Epac/cAMP pathway and the MAPK pathway mediate hCG induction of leptin in placental cells, PLoS One 7 (10) (2012) e46216.

[75] V. von Bulow, S. Dubben, G. Engelhardt, S. Hebel, B. Plumakers, H. Heine, L. Rink, H. Haase, Zinc-dependent suppression of TNF-alpha production is mediated by protein kinase A-induced inhibition of Raf-1, I kappa B kinase beta, and NF-kappa B, J. Immunol. 179 (6) (2007) 4180–4186.